Title: Elucidation of the downfield spectrum of human brain at 7T using multiple inversion recovery delays and echo times

Nicole D. Fichtner[1,2,3], Anke Henning[3,4], Niklaus Zoelch[3], Chris Boesch[1], Roland Kreis[1]

1 Depts. Radiology and Clinical Research, University Bern, Bern, Switzerland; 2 Graduate School for Cellular and Biomedical Sciences, University Bern, Bern, Switzerland; 3 Institute for Biomedical Engineering, UZH and ETH Zurich, Zurich, Switzerland; 4 Max Planck Institute for Biological Cybernetics, Tuebingen, Germany

Corresponding author: Roland Kreis, Ph.D., University of Bern, Pavilion 52, Inselspital, CH-3010 Bern, Switzerland.
E-mail: roland.kreis@insel.ch

Word count: 4,707

Abstract:

Purpose: Characterization of the downfield spectrum at 5-10ppm, which is less well characterized than upfield, in human brain at a high magnetic field of 7T. Knowledge of relaxation parameters is of interest for spectroscopy as well as chemical exchange dependent saturation transfer experiments.

Methods: This work includes water-suppressed echo time and inversion recovery series in healthy volunteers to investigate, respectively, T_2 and T_1 values of peaks in grey matter at 7T. The spectra were fitted in a 2D fashion to a heuristic model of a series of Voigt lines, and the relaxation times were obtained for twelve peaks of interest.

Results: Mean T_2's averaged over the volunteers ranged from 24-158ms, while mean T_1's ranged from 0.22-2.40s. Spectra of specific inversion and echo times reveal superposition of the amide peaks of NAA with short T_2 and an inhomogeneously broadened component with longer T_2.

Conclusions: T_2 values were shorter than expected for most peaks, while T_1 values had a very large range; shorter relaxation times for some peaks suggests the presence of macromolecules. Most of the larger peaks seem to be composed of overlapping components, as the Gaussian widths in the Voigt lineshape descriptions are larger than expected based on field inhomogeneities.

Key words: proton MR spectroscopy; 7T; human brain; metabolites; T_1 relaxation time; T_2 relaxation time

Introduction:

Magnetic resonance spectroscopy (MRS) is a noninvasive tool to measure changes in metabolite concentrations that are often not reflected by abnormalities in MR images, or in other non-invasive imaging modalities. Thus far, the characterization and quantification of the upfield side of the ^{1}H MR spectrum, to the right of the water peak, has been the focus at lower field strengths as well as higher field strengths, up to 9.4 T in human brain in vivo measurements (1-3). However, the downfield side of the spectrum, to the left of the water peak, is less well-characterized. While there are technical challenges associated with measuring downfield spectra, including lower signal to noise ratio and several exchanging peaks, it would be beneficial to determine both the identity of the visible peaks as well as their characteristics such as concentration, T_1, and T_2.

Downfield metabolites such as adenosine triphosphate (ATP), homocarnosine, glutathione, phenylalanine, and glutamine (4) may be of interest in metabolism and disease. For example, ATP is present upfield, but close to the water resonance, complicating quantification. Other interests in downfield spectra involve metabolites which exchange with water and can be measured using chemical exchange dependent saturation transfer (CEST) experiments; spectroscopy experiments on exchanging species may aid in improving CEST quantification.

Downfield MR spectroscopy has been performed in animals at up to 11.74 T, with tentative assignments of peaks including NAA at 7.8 ppm, NAD+ in the 8.7 – 9.5 ppm region, and proteins at 8.3 ppm, and with a focus on exchanging peaks (5-7). In humans, experiments have been run downfield at field strengths up to 7 T, investigating various resonances including NAA and several other peaks in the range from 5.9 ppm to 8.6 ppm (8-12). While some peaks are assigned to various metabolites based on expected resonances as well as water exchange (WEX) filter experiments (13), others remain unassigned and may be composed of multiple overlapping resonances. T_1 and exchange measurements have only investigated six of the visible peaks between 6.5 ppm and 8.6 ppm (8), and there is only a single report on T_2's of downfield peaks from a study at 1.5T (11) and preliminary accounts of T_2 attenuation at 1.5 and 3T (10), as well as 7T (9). These parameters may aid in designing further experiments to separate out the various potentially overlapping peaks of different metabolites downfield, as well as to determine the presence of any macromolecular baseline.

Performing MRS measurements at higher field strengths improves SNR and spectral resolution. However, several disadvantages remain and need to be accounted for, including a shorter T_2 of

the metabolites and higher radiofrequency power deposition. A shorter T_2 leads to line broadening as well as a smaller signal at longer echo times; therefore, a sequence with a short echo time is necessary at higher fields, particularly if one wishes to evaluate the T_2 of the metabolites.

In the current study, a STimulated Echo Acquision Mode (STEAM) sequence was used with a short echo time and a long repetition time to minimize the specific absorption rate, or amount of energy deposited. The focus of these experiments was to obtain T_1 and T_2 estimates downfield in grey matter (GM) in vivo in human subjects at 7 T and thereby to distinguish between small metabolite resonances and contributions from macromolecules. Increased knowledge about the downfield peaks can aid in the development of a model for better quantification in the future, and enable downfield measurements to be more easily used to determine changes in the brain due to metabolism or disease.

Methods:

Subjects

For the echo-time series, twelve healthy adults aged 21-49 years (mean 28 years) with no history of neurologic or psychiatric disorders were recruited, and for the inversion recovery series, ten healthy adults aged 21-49 years (mean 27 years) were recruited. Written, informed consent was obtained according to the local institutional ethics review board. Spectra from two subjects for the echo-time series were not included in the analysis due to excessive line broadening, most likely due to motion over the duration of the scan sessions.

MRS Data Acquisition

Subjects were scanned on a 7 T Philips Achieva MR system with a quadrature transmit/receive visual cortex surface coil (RAPID Biomedical, Rimpar, Germany). Sagittal, axial, and coronal T_2-weighted images were used for prescription of a mostly grey matter voxel of size 4.0 x 2.0 x 2.0 cm^3 in the visual cortex at the back of the head, avoiding major blood vessels.

Second-order local projection based B_0 shimming was applied using a Philips implementation (14) of FASTmap, FASTERmap, and FASTESTmap (15-18). Water suppression was achieved using an eight-pulse variable pulse power and optimized relaxation delays (VAPOR) (19) scheme (sinc-Gauss pulses, bandwidth 250 Hz) prior to the localization sequence. The VAPOR delays were 150, 100, 122, 105, 102, 61, and 67 ms for the seven pre-localization pulses. The

acquisition bandwidth was 4000 Hz, the number of data points acquired 2048, the RF pulse centre frequency was set at 7.5 ppm, and a 16-step phase cycling scheme was used.

The TE series was acquired using STEAM with a mixing time TM of 26.0 ms and a repetition time (TR) of 4000 ms. A series of echo times: 13.0, 23.4, 34.7, 46.8, 60.0 ms was acquired in each of the subjects, 256 averages per TE were collected in blocks of 64 averages each, and 4 unsuppressed water spectra were also acquired per block.

The IR series was acquired also using STEAM with a TM of 26.0 ms, a TE of 13.0 ms, and a TR of 7000 ms; the inversion times were 45, 150, 290, 580, 800, 1200, 2500, 4000, and 6000 ms. The nonselective trapezoidal adiabatic inversion pulse was interleaved with the VAPOR water suppression pulses as in Ref. (20), and the inversion times were calculated such that there was no overlap between the inversion pulse and any VAPOR pulse. At each inversion time, 64 averages were acquired, and 4 unsuppressed water spectra were also acquired.

MRS Data Analysis

All data were saved in the Philips raw data format, and exported and reconstructed in Matlab (MATLAB and Statistics Toolbox Release 2014b, The MathWorks, Inc., Natick, Massachusetts, United States). Oversampling was removed, a DC offset correction was applied, and the data were averaged, all using the ReconFrame framework (GyroTools LLC, Zurich, Switzerland). Following that, further processing in Matlab was done separately from ReconFrame, starting with 0^{th} order phase adjustment and then frequency alignment of the various data sets for each set of experiments using cross-correlation. For the TE series, the four sets of 64 averages for each echo time were then averaged together. For both TE and IR series, the data were then eddy current corrected using the corresponding data from non-water-suppressed scans (21). Data sets were aligned between volunteers, and were then also averaged to create a model spectrum with higher signal to noise ratio (SNR). The same processing was performed on the unsuppressed water data as for the water-suppressed spectra, including self-eddy current correction.

The overall averaged data sets from both series were used to develop a model in FiTAID (22); using the averaged data sets, prior knowledge was defined with twelve peaks in the 5 to 9 ppm region (see Figure 1). The peaks from N-acetylaspartate (NAA) at 7.82 ppm and α-glucose (Glc) at 5.22 ppm (4) were defined as binary patterns, as modeled in VESPA (23) based on the known spin systems. Homocarnosine (hCs) was also defined at two locations, 7.05 and

8.02 ppm as suggested by literature (24). Several other lines were used in the model, including one for an artifact at approximately 5.6 ppm which appeared in three of the TE series subjects, as well as a line to fit the residual water, a very broad line centered at the water frequency for any baseline effects, and another numeric pattern to account for the upfield spectra.

Subsequently, the individual volunteers' IR and TE data sets were fitted simultaneously within each time series using Voigt lineshapes, where the simultaneous fit mode helped to overcome the very low SNR for some of the peaks in individual spectra, particularly at long TE or the inversion null. Fitted parameters included peak area, offset, phase, Lorentz width (=$1/(\pi T_2)$), Gaussian width, and relaxation constant R_1 (=$1/T_1$), with the FiTAID model assuming full 180° inversion for the IR series. The NAA doublet peaks were linked such that their offset, area, Lorentz width, Gaussian width, and relaxivity R_1 were the same. The two homocarnosine peaks were also linked such that their areas, Lorentz width, and R_1 were identical, and the difference in their offset was fixed. Phase for the downfield spectrum was fixed and not varied between peaks; relative offsets between peaks were also not allowed to change from what had been found for the averaged data. Similarly for the Gauss width components; they remained at what was found for the averaged data, except that an additional Gauss broadening term was allowed to vary and adapt for different shim settings in the different data sets. In addition, for the TE series, R_1 was fixed based on the averaged data while the Lorentz width was fitted. Inversely, for the IR series, the Lorentz width was fixed based on the fit of the averaged data and R_1 was fitted. Fitting errors for all estimated parameters were determined as Cramer-Rao Lower Bounds (CRLB) (25).

Unsuppressed water data were also fitted in FiTAID, using a two-line model to account for the presence of cerebrospinal fluid (CSF). Metabolite concentrations were calculated using the relaxation-corrected water areas and a grey matter water concentration of 0.83 g/ml (26).

Not all of the fits were considered reliable; those with areas varying further than two standard deviations from the median area of the corresponding peak over all the individuals or those which hit the upper or lower limit of Lorentz width or R_1, for the T_2 or T_1 series, respectively, were removed. In addition, in some cases, the Fisher information matrix became singular and non-invertible, and singular value decomposition was used to calculate a pseudo-inverse of the matrix. The reason for the singularity was little/no influence of a parameter on the model (e.g. in some cases the Lorentz width was not relevant since the amplitude of the peak was extremely

small); parameters with infinite CRLB values were therefore also excluded from the final calculations.

For the calculation of the mean T_2 values and concentrations from the TE series, the α-glucose peak had two data sets removed; for homocarnosine, three were removed; the 5.73 ppm peak was poorly fitted and had eight data sets removed, while the 5.97 ppm peak had three removed and the 6.11 ppm had nine removed due to both infinite CRLB and in some cases hitting the limit for the Lorentz width. The 6.81 ppm and 8.08 ppm peaks had only one removed each, and the 7.06 ppm, 7.29 ppm, 8.0 ppm, and NAA peaks had none removed. For the calculation of the mean T_1 values and concentrations from the IR series, α-glucose and the 5.73 ppm peak had two data sets removed; homocarnosine, the 5.97 ppm, and the 6.81 ppm peak each had one data set removed, and the 6.11 ppm peak had five removed; the remaining peaks had none removed. Mean and standard deviations were calculated for the remaining data sets.

Results:

The average TE and IR series spectra used to create the model in FiTAID are shown in Figure 2. The appropriateness of the heuristic signal model can be judged from Figure 1, where the individual components are illustrated for the averaged short TE spectrum without inversion. Substantial inhomogeneous broadening (i.e. considerably larger Gauss component in the individual Voigt lines than found for the narrowest peaks of NAA and Glc) was found for peaks b to e with additional Gaussian broadening of 17 to 40 Hz (and the very broad baseline peak a).

Relaxation times and concentrations for all components were determined from the individual data sets. Mean T_2 estimates for metabolites were determined to be in the range of 24.3 to 158 ms, while mean T_1 values were in the range of 0.17 to 2.40 s. The mean water T_2 for the GM component was calculated to be 39.2 ± 3.1 ms (SD), while the mean water T_1 for GM was found to be 1.66 ± 0.09 *s*. The estimates for relaxation parameters and metabolite concentrations are shown in Tables 1 and 2, as mean and SD over the individuals, and the mean of the individual fitting uncertainties is also included. In addition, relaxation parameters and concentrations are given for the average spectra, useful in particular as comparison for the smaller peaks. Most of the peaks are unassigned and are therefore identified according to a label as shown in Figure 1. Examples of an individual fit with the spectrum and residuals are shown in Figure 3. Plots indicating the entire range of results for T_1 and T_2 values, including the outliers removed before determining mean values, are given in Figure 4.

Discussion:

The results from the current study provide T_1 and T_2 values at 7 T, as well as concentration estimates for twelve peaks of interest downfield from a mostly grey matter voxel. The relaxation parameters discussed here provide information on more peaks than the six previously shown downfield in human brain at 3 T (8) and relaxation differences point at the presence of macromolecular components.

As can be seen from the CRLB and the standard deviations over the cohorts in Tables 1 and 2, the results for several peaks were very consistent, including the NAA peaks and several of the larger downfield peaks. Other peaks were more difficult to fit, such as the α-glucose, suffering from additional baseline effects due to its proximity to the water peak, and several of the smaller peaks, which were more difficult to see in the individual spectra compared to the averaged spectra. These gave a wider range of results for T_1, T_2, and concentrations.

Metabolite concentrations

The metabolite concentrations found for the known downfield peaks for the most part match very well to the literature values (1,3,4). The narrow NAA amide doublet corresponds to a concentration of 10.5 mM from the T_2 measurements and a concentration of 9.9 mM from the T_1 measurements, agreeing with each other and literature values of an average of 10.3 mM (4). Homocarnosine, which was included in the model as two peaks based on prior knowledge as it overlaps with other peaks, yielded a concentration of 0.27 mM from the T_1 measurements and 0.39 mM from the T_2 measurements. This is close to the literature values of 0.23 mM (4) and 0.3-0.4 mM (24,27). The literature suggests a concentration of 0.5 mM for α-glucose (12), which is comparable to the concentrations of 0.77 mM and 0.44 mM obtained in the current study, although it should be noted that the α-glucose peak may be somewhat affected by the transition band of the 250 Hz-bandwidth water suppression pulses. Other peak concentrations are more difficult to discuss, as some of them are likely to be composed of various metabolites and remain unassigned, as discussed later.

Water T_1 and T_2

The mean water T_1 and T_2 were found to be 1.66 ± 0.09 s and 39.2 ± 3.1 ms, respectively. The T_1 is lower than the recently found 2.0s for grey matter at 7 T (2); however, in that case the CSF was not accounted for when fitting the grey matter voxel, and may have led to a larger T_1 than measured here, although imaging studies suggest a range of T_1 values somewhere in between

the two results (28). The T_2 is in the expected range for grey matter at higher fields, although still slightly below the average literature values found for 7 T which are mostly above 41 ms (1,29).

Metabolite relaxation values

Compared to the 3 Tesla T_1 values found by MacMillan et al (8), the values found at 7 T are, for the most part, substantially higher. However, the 3 T results were found through modeling of exchange experiments (selective inversion of water peak), in contrast to the non-selective inversion recovery experiments run at 7 T, and cannot be directly compared. Some of the peaks have fairly large standard deviations, either because they arise from small features that are difficult to fit in individual spectra or because their T_1 is so short that the choice of inversion times was not ideal to determine them accurately.

There are few publications discussing downfield T_2 values; one set of experiments done at 1.5 T, however, does list a T_2 value for NAA of 17 ms and for the 7.3 ppm peak of 52 ms (11). These values differ somewhat from the values found at 7 T, but are of a similar order of magnitude; furthermore, their work also indicates a second component of the NAA peak at 8.0 ppm, similar to the findings of an extra component at 7.87 ppm at 7 T. A comparison to upfield shows that most of the downfield T_2 values found are significantly shorter, at approximately 24-43 ms, than those found at 7 T for upfield metabolites, which were mostly within a range of 60-200 ms (1). However, some of the peaks have values in a similar range above 100 ms, such as homocarnosine, the 5.97 ppm peak (peak g in Figure 1), and α-glucose, with slightly less accurate fits, as mentioned earlier. It should be noted that Marjanska et al. (1) found different T_2 values for different areas in the brain; direct comparisons therefore may depend on which area of the brain is being investigated. The longer T_2 for the α-Glc peak is in line with expectations based on work by Gruetter et al (12) at 4 T.

For the NAA amide peak, the mean T_1 was found to be 1.84 s at 7 T, while at 3 T the median T_1 was estimated from the inversion transfer to be 0.53 s, which is a larger difference than that typically seen between 3 T and 7 T for upfield peaks. The difference may partly be due to the different experiment types and partly due to the fact that at 3 T, the broader NAA resonance fitted for T_1 included the shoulder that was fitted separately at 7 T, with a T_1 of 0.85 s. On the other hand, the NAA amide N-H peak was found to have a very short T_2 of 28.0 ± 2.4 ms, with consistent fits across all subjects, which is in strong contrast to the upfield spectrum, where the NAA acetyl group has one of the longer T_2 values also at 7 T, for e.g. 132 ms for the methyl

peak and 90 ms for the aspartate CH_2 group in the occipital lobe (1). Exchange could be expected to play a role, leading to an apparently shorter T_2; however, MacMillan et al. (8) found that the NAA peak has a very low exchange rate of 0.5 Hz, which would not contribute much to the apparent T_2. Alternatively, the apparent T_2 of the amide peak may well be dominated by scalar relaxation mediated by J-coupling (expected to be on the order of 60 Hz) to the fast relaxing nitrogen-14 in NAA. To pinpoint this effect is, however, beyond the scope of this work, but may be of considerable interest for in vivo amide peaks in general.

A peak at 7.87 ppm (peak b in Figure 1) contributes a broad shoulder to the larger NAA peak; it has a shorter T_1 than many of the other peaks but a longer T_2 than the NAA peak itself. It can be seen in Figure 2 that it recovers faster in the IR series than NAA, with a broader peak visible at TI = 1.20 s. To better visualize that there is indeed an additional component at 7.87 ppm, a scaled version of these traces is given in Figure 5, where the 7.87 ppm peak appears clearly shifted and broader than the NAA peak that dominates and lines up across the other plotted traces. Given that this broad peak at 7.87 ppm and several other peaks were described by Voigt lines with Gaussian components that are much larger than the contribution from local B_0-inhomogeneity indicates per se that these peaks consist of multiple contributing components and the determined relaxation times can only give a rough estimate for the main contributors at these chemical shift positions. It also explains why a broad component, like the one at 7.87 ppm, can be associated with a longer T_2 than the narrower NAA amide peak, which even consists of a J-coupling doublet.

Knowledge of the relaxation values is also of interest for determining the presence of macromolecules. The peak at 6.81 ppm (peak e) has a very short T_1 of 0.47 s compared to many of the other well-fitted peaks (not including the 6.11 ppm (peak f) and 5.73 ppm (peak h) peaks, which were small and more difficult to fit accurately). The shorter T_1 compared to upfield T_1's and to other downfield peaks, in addition to a short T_2 of 24.4 ms indicates the likely presence of a macromolecular contribution to the peak. The other two peaks at 7.06 and 7.29 ppm (peaks d and c) also have short T_1's of 0.74 s and 0.70 s respectively, higher than at 3 T but only slightly higher than the macromolecular T_1 of 0.43 s found upfield at 7 T (2), and therefore may also contain macromolecular components. The relatively short T_2 values of 35.9 ms and 30.4 ms for the 7.06 ppm and 7.29 ppm peaks, respectively, are in line with the potential presence of macromolecules.

Comparing T_1 values between field strengths is more difficult for the remaining peaks, as the area between 8.1-8.5 ppm is strongly affected by exchange (amides), which was minimized in the 3 T experiments without water pre-saturation, and the 3 T experiments did not investigate peaks as close to the water peak as those at 7 T.

Peak assignments

Several peaks such as those from NAA and α-glucose have been unambiguously labeled in previous experiments (30); however, many of the peaks investigated in the current study remain unlabeled. Tentative peak assignments have been given for downfield peaks previously by Henning et al. (9); these labels were based on expected metabolite resonances found in the literature. Further labeling or confirmation of peaks is not yet possible with the results obtained in this study; however, some suggestions can be made and others ruled out. NAA and α-glucose remain well-known as downfield peaks at 7.82 ppm and 5.22 ppm (4). Homocarnosine was found at both 7.05 ppm and at 8.02 ppm, corresponding to what had been obtained in Ref. (24) after vigabatrin treatment (7.05 and 8.02 ppm). The peak at 5.73 ppm may be labeled as urea, based on a recent publication (31) and a measured concentration of 2.6 mmol/kg urea in human brain extracts (32).

The peaks at 8.1-8.5 ppm (peak a) are partly due to amide protons which exchange with water and have been shown in WEX experiments (13); in the current case, water is suppressed, leading to smaller or nonexistent peaks. These peaks may thus arise partially from amide protons of peptides/proteins (13) but also from various other metabolites such as glutathione or homocarnosine. Two peaks from ATP are expected in this ppm range (8.2 and 8.5 ppm), arising from the adenosine moiety. However, if fully visible and present at a level of ~3 mM (4), they should actually be considerably more prominent than what is observed in our spectra. These protons are not expected to exchange directly with water; any decrease in signal may be due to a nuclear Overhauser effect as reported for the aromatic signals from proteins (33) or T_2 shortening because of the specific compartmentation or chemical reactions ATP is involved in. To arrive at the low spectral intensities seen in our spectra, T_2's would have to be considerably shorter than what was measured for peak a. The same holds for the potential ATP resonance at 6.12 ppm. It is too small if ATP were fully visible and too narrow to represent T_2-shortening and signal loss.

Amine groups also resonate downfield from water. Candidate peaks include ATP at 6.76 ppm, creatine at 6.65 ppm, glutamine at 6.82 and 7.53 ppm, homocarnosine at 6.40 ppm, and

phosphocreatine at 6.58 and 7.30 ppm. However, as amines tend to exchange rapidly with water (34-36), these resonances and any amines from other metabolites such as glutamate and GABA are not expected to be visible in these water-suppressed experiments. Similarly, the amide peaks of glutathione identified at 8.27 and 8.48 ppm by Grande et al. (37) in cell suspensions are expected to be strongly attenuated due to exchange. (These assignments contrast with Ref. (4), where the glutathione peaks were assigned to 7.15 and 8.18 ppm, but Grande's assignments are more in line with earlier high resolution work (38)). MacMillan et al.'s experiments at 3 T show low exchange rates for the 7.06 and 7.29 ppm peaks (peaks d and c, respectively), which may indicate either a small component which exchanges or only slowly exchanging species which may still be visible.

Other resonances expected or previously reported to be visible in the downfield spectrum include histidine, tryptophan, tyrosine, and phenylalanine, with all of them present at a low concentration only (<0.1 mmol/kg_{ww}) but the latter four with 4-5 protons potentially cumulating to a small detectable signal. Simulations (not shown) were performed for the 7 T case and indicate that these metabolites are too low in concentration to account for substantial parts of the larger peaks in the 6.8-7.3 ppm region (peaks c, d, and e).

Limitations

An ideal experiment would have no suppression effects on the metabolites from exchange with suppressed water; however, the ability to run metabolite cycling experiments to avoid water suppression was limited by scanner instabilities. Comparison of water-suppressed and non-water-suppressed spectra at 3 T (8) suggests that the water suppression sequence has only substantial effects for a few of the visible peaks; any peaks affected by very fast exchange would not be visible from the metabolite cycling sequence even without water suppression due to broadening effects as well as relaxation or exchange after the inversion pulse. Similar effects from water suppression would be expected at 7 T, although faster exchanging peaks would be expected to be smaller or no longer visible due to the longer VAPOR water suppression duration. There could be some effects due to exchange on some of the remaining peaks, leading to a shorter T_2 than expected; however, the peaks with the highest exchange rates were not visible enough for quantification in these experiments. NAA, as mentioned earlier, is likely not affected due to a very low exchange rate of 0.5 Hz (8). The presence of exchanging peaks/metabolites has been demonstrated in experiments such as WEX (13), where the amide

protons appeared to be the fastest exchanging, and others had slower exchange rates, and therefore were less impacted by water suppression.

In theory, many resonances should be visible downfield; however, in practice, effects including exchange and – as seen from the present results – short T_2 are likely to eliminate some of the metabolites as contributors to the visible signal. A further limitation is the simplification of the spectral fit model, which was developed to characterize visible peaks but not necessarily all contributing resonances individually, as many of the peaks are likely due to various overlapping resonances. This overlap creates the broader peaks visible in the 6.8-7.3 ppm range; some of the metabolites with lower concentrations may be contributing to a larger overall peak.

Three spectra in the TE series have an artifact, appearing as a dip in the spectrum, at approximately 5.6 ppm (denoted by a * in Figure 1); this artifact is less obvious in the averaged spectrum than in the individual spectra but was accounted for in the fitting.

Conclusions

This paper presents first estimates of T_1 and T_2 at 7 T downfield in grey matter for twelve peaks. As downfield spectra have not been well characterized at ultra-high field in humans in vivo, this paper presents initial results with the aim to improve the characterization and labeling of the peaks.

T_2 values were shorter than expected for most peaks, while T_1 values had a very large range, suggesting the presence of macromolecules for some of the peaks with shorter T_1's and T_2's, such as those at 6.81, 7.06, and 7.29 ppm. The larger peaks were well fitted by the model, while the smaller peaks were clearly present but difficult to fit in individual spectra.

Acknowledgements

This work is supported by the Swiss National Science Foundation (SNSF #320030-156952).

References

1. Marjanska M, Auerbach EJ, Valabrègue R, Van de Moortele P-F, Adriany G, Garwood M. Localized 1H NMR spectroscopy in different regions of human brain in vivo at 7 T: T2 relaxation times and concentrations of cerebral metabolites. NMR Biomed 2012;25:332-339.

2. Xin L, Schaller B, Mlynarik V, Lu H, Gruetter R. Proton T1 relaxation times of metabolites in human occipital white and gray matter at 7 T. Magn Reson Med 2013;69:931-936.

3. Deelchand DK, Van De Moortele PF, Adriany G, Iltis I, Andersen P, Strupp JP, Vaughan JT, Ugurbil K, Henry PG. In vivo 1H NMR spectroscopy of the human brain at 9.4 T: initial results. J Magn Reson 2010;206:74-80.

4. Govindaraju V, Young K, Maudsley AA. Proton NMR chemical shifts and coupling constants for brain metabolites. NMR Biomed 2000;13:129-153.

5. Mori S, Eleff SM, Pilatus U, Mori N, van Zijl PC. Proton NMR spectroscopy of solvent-saturable resonances: a new approach to study pH effects in situ. Magn Reson Med 1998;40:36-42.

6. De Graaf R, Sacolick L, Rothman D. Water and metabolite-modulated MR spectroscopy and spectroscopic imaging. In Proceedings of the 14th Meeting of ISMRM, Seattle, USA, 2006. p. 3063.

7. de Graaf RA, Behar KL. Detection of cerebral NAD+ by in vivo1H NMR spectroscopy. NMR Biomed 2014;27:802-809.

8. MacMillan EL, Chong DGQ, Dreher W, Henning A, Boesch C, Kreis R. Magnetization exchange with water and T1 relaxation of the downfield resonances in human brain spectra at 3.0 T. Magn Reson Med 2011;65:1239-1246.

9. Henning A, Fuchs A, Boesch C, Boesiger P, Kreis R. Downfield spectra at ultrahigh field. In Proceedings of the 16th Meeting of ISMRM, Toronto, Canada, 2008. p. 777.

10. Kreis R, Boesch C, Vermathen P. Characterization of the downfield part of the human cerebral 1H MR spectrum at 3 T. In Proceedings of the 14th Meeting of ISMRM, Seattle, USA, 2006. p. 2636.

11. Vermathen P, Capizzano AA, Maudsley AA. Administration and (1)H MRS detection of histidine in human brain: application to in vivo pH measurement. Magn Reson Med 2000;43:665-675.

12. Gruetter R, Garwood M, Ugurbil K, Seaquist ER. Observation of resolved glucose signals in 1H NMR spectra of the human brain at 4 Tesla. Magn Reson Med 1996;36:1-6.

13. van Zijl PC, Zhou J, Mori N, Payen JF, Wilson D, Mori S. Mechanism of magnetization transfer during on-resonance water saturation. A new approach to detect mobile proteins, peptides, and lipids. Magn Reson Med 2003;49:440-449.

14. Hock A, Fuchs A, Boesiger P, Kollias SS, Henning A. Electrocardiogram-triggered, higher order, projection-based B0 shimming allows for fast and reproducible shim convergence in spinal cord 1H MRS. NMR Biomed 2012;26:329-335.

15. Gruetter R, Boesch C. Fast, Noniterative Shimming of Spatially Localized Signals. In vivo Analysis of the Magnetic Field along Axes. J Magn Reson 1992;96:323-334.

16. Gruetter R. Automatic, localized in vivo adjustment of all first- and second-order shim coils. Magn Reson Med 1993;29:804-811.

17. Shen J, Rycyna RE, Rothman DL. Improvements on an in vivo automatic shimming method [FASTERMAP]. Magn Reson Med 1997;38:834-839.

18. Gruetter R, Tkac I. Field mapping without reference scan using asymmetric echo-planar techniques. Magn Reson Med 2000;43:319-323.

19. Tkac I, Starcuk Z, Choi IY, Gruetter R. In vivo 1H NMR spectroscopy of rat brain at 1 ms echo time. Magn Reson Med 1999;41:649-656.

20. Fuchs A, Luttje M, Boesiger P, Henning A. SPECIAL semi-LASER with lipid artifact compensation for 1H MRS at 7 T. Magn Reson Med 2013;69:603-612.

21. Klose U. In vivo proton spectroscopy in presence of eddy currents. Magn Reson Med 1990;14:26-30.

22. Chong DGQ, Kreis R, Bolliger C, Boesch C, Slotboom J. Two-dimensional linear-combination model fitting of magnetic resonance spectra to define the macromolecule baseline using FiTAID, a Fitting Tool for Arrays of Interrelated Datasets. Magn Reson Mater Phy 2011;24:147-164.

23. Soher B, Semanchuk P, Todd D, Steinberg J, Young K. VeSPA: Integrated applications for RF pulse design, spectral simulation and MRS data analysis. In Proceedings of the 19th Meeting of ISMRM. Montreal, Canada, 2011. p. 1410.

24. Rothman DL, Behar KL, Prichard JW, Petroff OA. Homocarnosine and the measurement of neuronal pH in patients with epilepsy. Magn Reson Med 1997;38:924-929.

25. Cavassila S, Deval S, Huegen C, van Ormondt D, Graveron-Demilly D. Cramer-Rao bounds: an evaluation tool for quantitation. NMR Biomed 2001;14:278-283.

26. Whittall KP, MacKay AL, Graeb DA, Nugent RA, Li DKB, Paty DW. In vivo measurement of T_2 distributions and water contents in normal human brain. Magn Reson Med 1997;37:34-43.

27. Kish S, Perry T, Hansen S. Regional distribution of homocarnosine, homocarnosine-carnosine synthetase and homocarnosinase in human brain. J Neurochem 2006;32:1629-1636.

28. Marques JP, Kober T, Krueger G, van der Zwaag W, Van de Moortele P-F, Gruetter R. MP2RAGE, a self bias-field corrected sequence for improved segmentation and T1-mapping at high field. Neuroimage 2010;49:1271-1281.

29. Lopez-Kolkovsky AL, Mériaux S, Boumezbeur F. Metabolite and macromolecule T1 and T2 relaxation times in the rat brain in vivo at 17.2T. Magn Reson Med 2016;75(2):503-514.

30. Tkac I, Andersen P, Adriany G, Merkle H, Ugurbil K, Gruetter R. In vivo 1H NMR spectroscopy of the human brain at 7 T. Magn Reson Med 2001;46:451-456.

31. Watanabe T, Frahm J, Michaelis T. Amide proton signals as pH indicator for *in vivo* MRS and MRI of the brain--Responses to hypercapnia and hypothermia. Neuroimage 2016;133:390-298.

32. Moats RA, Lien YH, Filippi D, Ross BD. Decrease in cerebral inositols in rats and humans. Biochem J 1993;295:15-18.

33. Goerke S, Zaiss M, Kunz P, Klika KD, Windschuh JD, Mogk A, Bukau B, Ladd ME, Bachert P. Signature of protein unfolding in chemical exchange saturation transfer imaging. NMR Biomed 2015;28:906-913.

34. Kogan F, Hariharan H, Reddy R. Chemical Exchange Saturation Transfer (CEST) Imaging: Description of Technique and Potential Clinical Applications. Current Radiology Reports 2013;1:102-114.

35. Zaiss M, Bachert P. Chemical exchange saturation transfer (CEST) and MR Z-spectroscopy in vivo: a review of theoretical approaches and methods. Physics in Medicine and Biology 2013;58:R221-R269

36. Liepinsh E, Otting G. Proton exchange rates from amino acid side chains--implications for image contrast. Magn Reson Med 1996;35:30-42.

37. Grande S, Luciani AM, Rosi A, Guidoni L, Viti V. Identification of amide protons of glutathione in MR spectra of tumour cells. NMR Biomed 2008;21:1057-1065.

38. Schwartz C, Cutnell JD. One- and two-dimensional NMR studies of exchanging amide protons in glutathione. J Magn Reson 1983;53:398-411.

peak	MeanT_2 ± SD (ms)	CRLB (ms)	T_2 from average TE series (ms)	Mean T_1 ± SD (s)	CRLB (s)	T_1 from average IR series (s)
8.08ppm (a)	38.0 ± 7.1	5.9	37.4	0.22 ± 0.17	0.02	0.36
hCs	158 ± 87	173	318	2.40 ± 0.52	0.95	2.81
7.87ppm (b)	40.3 ± 6.3	7.6	44.2	0.84 ± 0.16	0.13	0.85
NAA	28.0 ± 2.4	1.5	28.7	1.84 ± 0.12	0.07	1.84
7.29ppm (c)	30.4 ± 4.8	2.8	30.4	0.70 ± 0.04	0.04	0.72
7.06ppm (d)	35.9 ± 5.4	4.6	35.9	0.74 ± 0.08	0.06	0.75
6.81ppm (e)	24.4 ± 1.8	2.9	25.5	0.47 ± 0.05	0.05	0.45
6.11ppm (f)	24.3 ± (N/A)	11.5	74.9	0.17 ± 0.08	0.16	0.23
5.97ppm (g)	111 ± 80.	138	88	1.91 ± 1.32	1.17	1.38
5.73ppm (h)	43.6 ± 28.8	28.5	22.4	0.36 ± 0.21	0.12	0.52
α-glucose	129 ± 84	111	269	1.71 ± 0.50	0.59	1.41
Water	39.2 ± 3.1	0.007	N/A	1.66 ± 0.09	0.0004	N/A

Table 1. Mean T_2 and T_1 values for the twelve peaks calculated from individual volunteers' fitted results. Standard deviations (SD) over all the results as well as mean CRLB from the results are shown. The T_2 and T_1 values from the average spectra over the volunteers from the TE and IR series, respectively, are also included.

Peak	Mean TE series conc. ± SD (mM)	CRLB (mM)	Conc. from avg TE series (mM)	Mean IR series conc. ± SD (mM)	CRLB (mM)	Conc. from avg IR series (mM)
8.08ppm (a)	9.02 ± 1.65	1.09	9.62	8.28 ± 1.85	0.46	9.68
hCs	0.39 ± 0.11	0.13	0.33	0.27 ± 0.06	0.06	0.53
7.87ppm (b)	3.02 ± 0.59	0.36	2.93	1.88 ± 0.30	0.26	1.14
NAA	10.5 ± 1.0	0.78	10.6	9.91 ± 0.98	0.36	9.85
7.29ppm (c)	4.81 ± 0.69	0.44	5.06	4.44 ± 0.37	0.18	4.58
7.06ppm (d)	3.35 ± 0.48	0.41	3.58	3.03 ± 0.31	0.18	3.96
6.81ppm (e)	3.72 ± 0.36	0.49	3.78	2.78 ± 0.21	0.18	3.87
6.11ppm (f)	0.47 ± (N/A)	0.18	0.11	0.11 ± 0.03	0.05	0.13
5.97ppm (g)	0.47 ± 0.20	0.15	0.44	0.36 ± 0.05	0.09	0.46
5.73ppm (h)	0.53 ± 0.43	0.26	0.24	0.81 ± 0.24	0.15	1.26
α-glucose	0.77 ± 0.30	0.27	0.46	0.44 ± 0.13	0.07	0.54

Table 2. Mean concentrations calculated from the individual results from the TE series and the IR series. Standard deviations (SD) over all the results as well as mean CRLB from the results are shown. The concentrations from the average spectra over the volunteers from the TE and IR series are also included.

Figure 1. Averaged spectrum from 10 volunteers at TE=13.0 ms shown in black, overlaid with the fit in red, and the individual basis peaks in dark blue; known peaks are shown in colour as labelled, with peaks fitted together shown in the same colour. Inset: representative voxel location shown in red overlaid on an image of a volunteer's brain acquired with a surface coil. Below the spectrum are the residuals for the fit. NAA, hCs, and Glc were included as known peaks, and NAA was fitted as a doublet. Unknown peaks are labelled with letters; j* corresponds to an artifact present in three subjects' data. Other metabolites with non-exchanging peaks resonating in this downfield region include phenylalanine, tryptophan, histidine, and tyrosine; simulations (not shown) indicate that even if summed together, these metabolites are too low in concentration to substantially account for the larger peaks in the 6.8-7.3 ppm region. The peak at 5.73 ppm can potentially be labeled as urea (31).

Figure 2. Average spectra over all volunteers. No filters applied. a) Average of the echo time series spectra for all 10 volunteers; echo times are shown to the left of the spectra. b) Average of the inversion recovery series spectra for all 10 volunteers; inversion times are shown to the left of the spectra.

Figure 3. a) Representative spectra from an individual volunteer for the TE series, b) the corresponding fitted spectra for the TE series, and c) the residuals from these fits. d) Representative spectra from an individual volunteer for the IR series, e) the corresponding fitted spectra for the IR series, and f) the residuals from the pertaining fits. No filters were applied to the data.

Figure 4. Plots for a) T_1 relaxation times and b) T_2 relaxation times for the twelve peaks downfield, from the fits of each individual volunteer. Black crosses are the included data points, red circles indicate data points removed from the calculations, and blue squares indicate the mean values. Note that for the T_1 relaxation times, three points at T_1 = 10 s were removed, two from the 6.11 ppm range and one from glucose.

Figure 5. Spectra indicating the presence of a component at 7.87 ppm, evidenced by the shift when comparing the NAA peak for the average IR series traces at TI = 45 (inverted), 1200, and 6000 ms. All traces are Gaussian apodized by 6 Hz. The TI = 1200 ms trace is shown in red, and is scaled up to match the NAA peaks of the other traces. As all the other peaks align between the traces, the shifted peak must therefore be a component other than NAA.

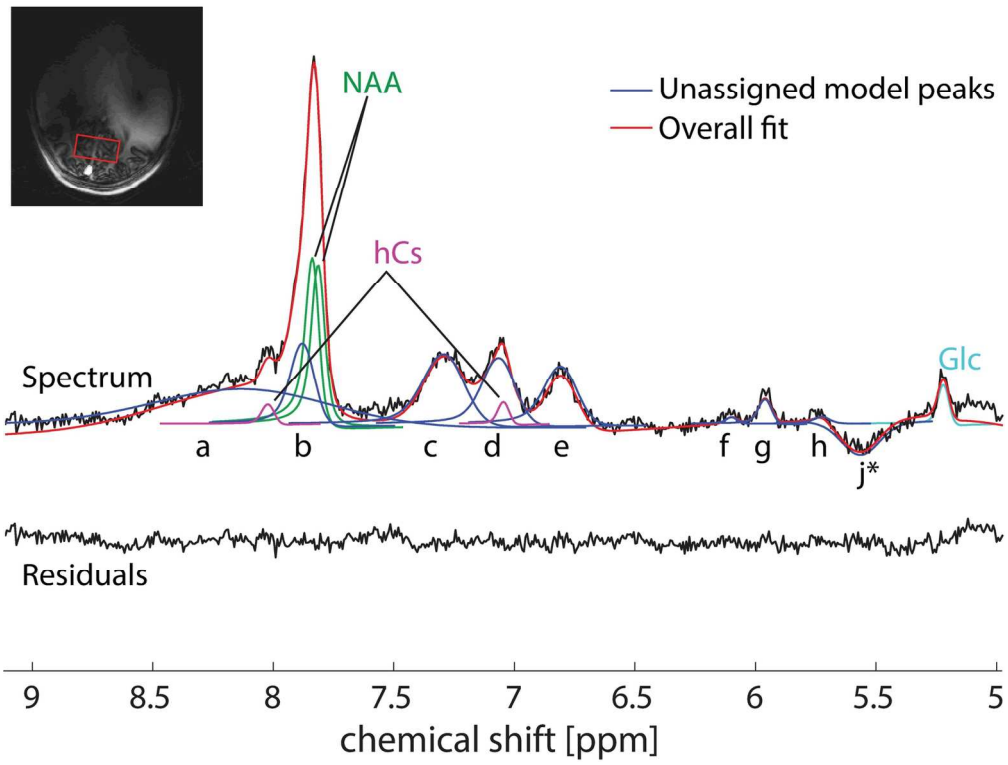

Figure 1. Averaged spectrum from 10 volunteers at TE=13.0 ms shown in black, overlaid with the fit in red, and the individual basis peaks in dark blue; known peaks are shown in colour as labelled, with peaks fitted together shown in the same colour. Inset: representative voxel location shown in red overlaid on an image of a volunteer's brain acquired with a surface coil. Below the spectrum are the residuals for the fit. NAA, hCs, and Glc were included as known peaks, and NAA was fitted as a doublet. Unknown peaks are labelled with letters; j* corresponds to an artifact present in three subjects' data. Other metabolites with non-exchanging peaks resonating in this downfield region include phenylalanine, tryptophan, histidine, and tyrosine; simulations (not shown) indicate that even if summed together, these metabolites are too low in concentration to substantially account for the larger peaks in the 6.8-7.3 ppm region. The peak at 5.73 ppm can potentially be labeled as urea (31).
150x114mm (300 x 300 DPI)

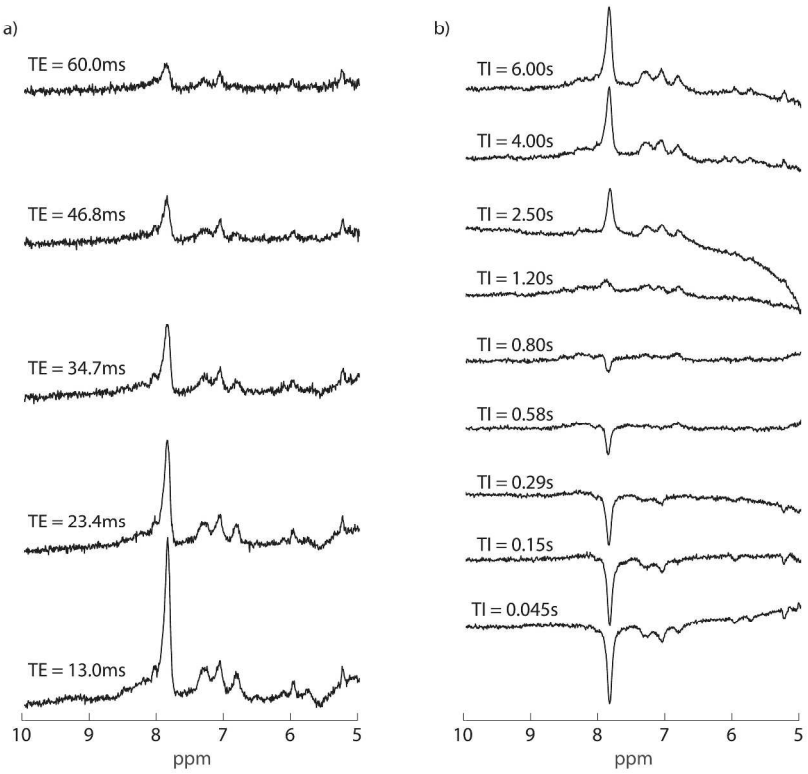

Figure 2. Average spectra over all volunteers. No filters applied. a) Average of the echo time series spectra for all 10 volunteers; echo times are shown to the left of the spectra. b) Average of the inversion recovery series spectra for all 10 volunteers; inversion times are shown to the left of the spectra.
288x256mm (300 x 300 DPI)

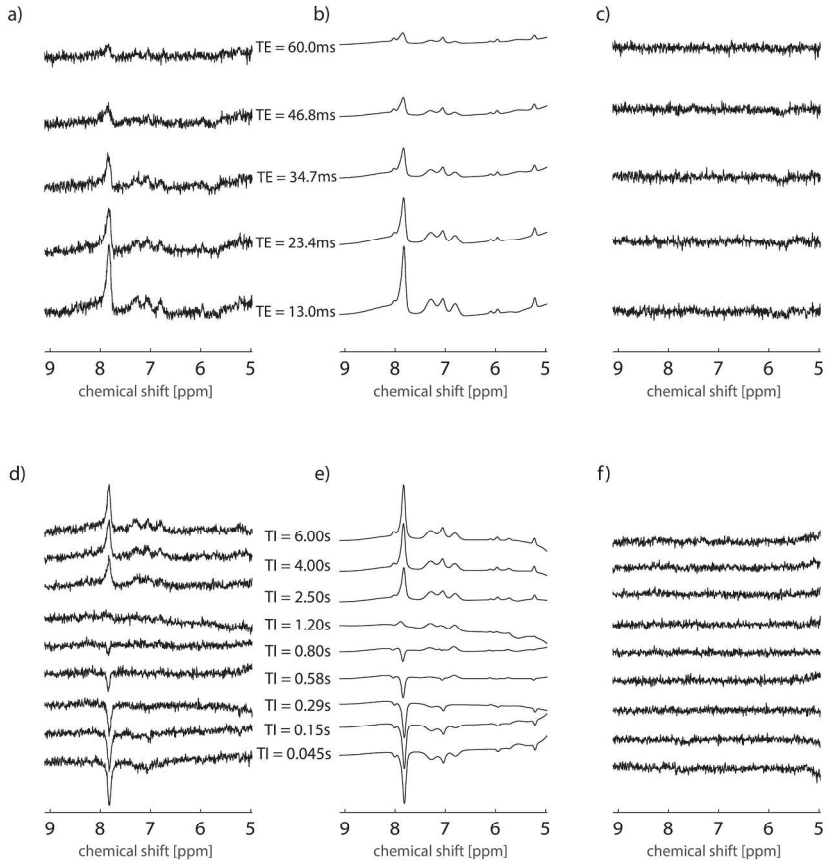

Figure 3. a) Representative spectra from an individual volunteer for the TE series, b) the corresponding fitted spectra for the TE series, and c) the residuals from these fits. d) Representative spectra from an individual volunteer for the IR series, e) the corresponding fitted spectra for the IR series, and f) the residuals from the pertaining fits. No filters were applied to the data.
238x231mm (300 x 300 DPI)

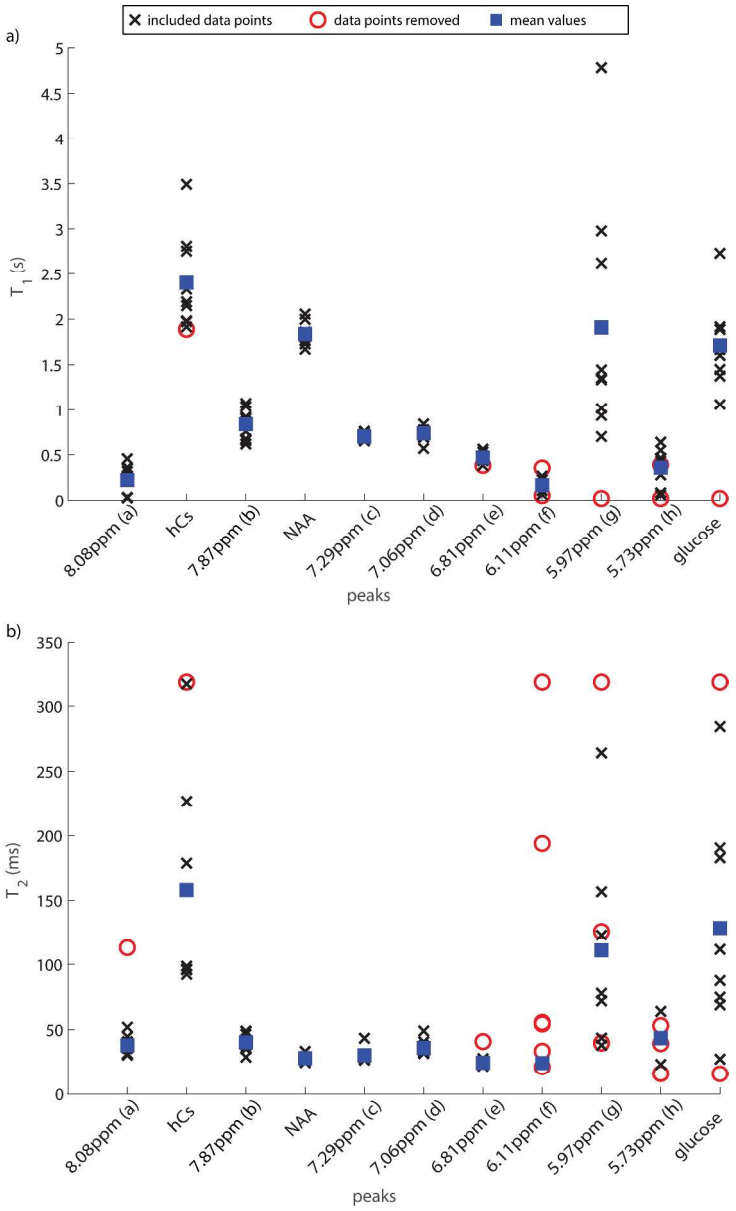

Figure 4. Plots for a) T1 relaxation times and b) T2 relaxation times for the twelve peaks downfield, from the fits of each individual volunteer. Black crosses are the included data points, red circles indicate data points removed from the calculations, and blue squares indicate the mean values. Note that for the T1 relaxation times, three points at T1 = 10 s were removed, two from the 6.11 ppm range and one from glucose.
348x576mm (300 x 300 DPI)

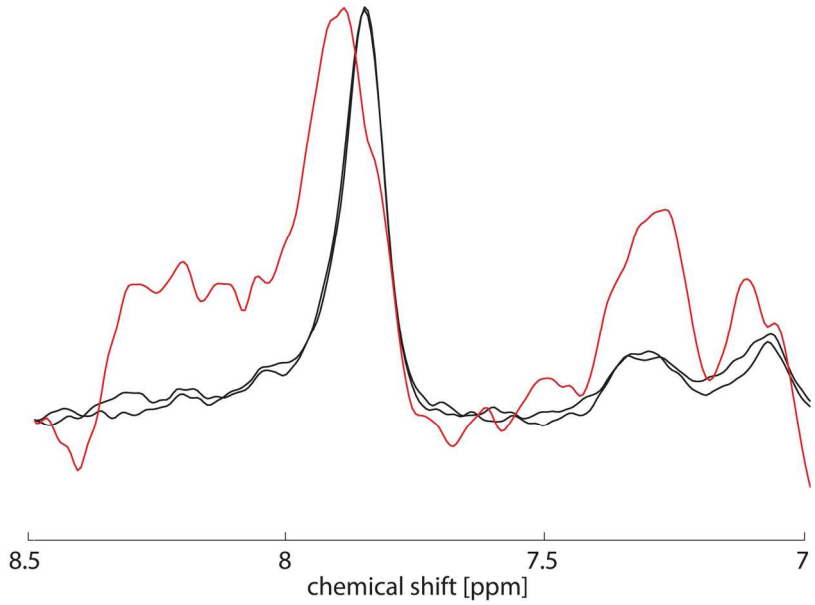

Figure 5. Spectra indicating the presence of a component at 7.87 ppm, evidenced by the shift when comparing the NAA peak for the average IR series traces at TI = 45 (inverted), 1200, and 6000 ms. All traces are Gaussian apodized by 6 Hz. The TI = 1200 ms trace is shown in red, and is scaled up to match the NAA peaks of the other traces. As all the other peaks align between the traces, the shifted peak must therefore be a component other than NAA.
160x106mm (300 x 300 DPI)